PERIÓDICO TCHÊ QUÍMICA
ARTIGO ORIGINAL

ESTIMATIVA DE SUPERFÍCIE ESPECÍFICA DE MCCC NO PROCESSO DE OXIDAÇÃO A BAIXA TEMPERATURA

CCCM SPECIFIC SURFACE ESTIMATION IN PROCESS OF LOW-TEMPERATURE OXIDATION

ОЦЕНКА УДЕЛЬНОЙ ПОВЕРХНОСТИ УУКМ В ПРОЦЕССЕ НИЗКОТЕМПЕРАТУРНОГО ОКИСЛЕНИЯ

POGODIN, Veniamin A.[1*]; ASTAPOV, Alexey N.[2]; RABINSKIY, Lev N.[3]

[1-3] Moscow Aviation Institute (National Research University), Department of Advanced Materials and Technologies for Aerospace Application, Moscow – Russian Federation

** Correspondence author*
e-mail: pogodin@yandex.ru

Received 22 December 2019; received in revised form 26 February 2020; accepted 19 March 2020

RESUMO

O processo de oxidação a baixa temperatura de materiais compósitos carbono-carbono (MCCC) com uma matriz de pirocarbono foi examinado. A oxidação em temperaturas de 450 a 700 °C é caracterizada por queima interna da fase de carbono, sem uma mudança perceptível no volume externo das amostras experimentais. Foi realizada análise de resistência à oxidação dos componentes estruturais do MCCC. O MCCC e a área superficial específica das fibras de carbono foram estimados pela adsorção a baixa temperatura de nitrogênio e criptônio usando o modelo Brunauer-Emmett-Teller e a teoria do modelo funcional da densidade. A distribuição do tamanho dos poros foi calculada pelo método semi-empírico de Horvath-Kawazoe. Um aumento significativo (cerca de 10 a 15 vezes) na área superficial específica do material compósito, juntamente com um aumento no volume livre ~ 5%, foi acompanhado por uma perda de peso total de cerca de 5%. Alterações específicas da área superficial ocorrem como resultado do ataque anisotrópico da superfície das fibras de carbono com a formação de microporos com uma faixa de diâmetro de 0,5–2,0 nm. Embora os macroporos sejam formados principalmente devido à oxidação do resíduo de pirólise do ligante termoendurecível, eles não contribuem para o aumento específico da superfície, mas apenas fornecem acesso aos microporos. A evolução da microporosidade leva a um aumento do grau de descontinuidade estrutural e, finalmente, à perda do limite de contato matriz-carga. Como resultado, um enfraquecimento geral das características mecânicas do material deve ser observado. Assim, a degradação oxidativa está intimamente relacionada ao aumento do espaço vazio. Um estudo de acompanhamento está em andamento. De fato, permanece uma questão em aberto: saber se o processo oxidativo ocorre diferentemente nos microporos de diâmetro inferior a 2 nm e como ele pode contribuir para o comportamento da resistência ao estresse oxidativo do CCCM.

Palavras-chave: *oxidação, microporos, BET, DFT, MCCC, área superficial específica*.

ABSTRACT

The low-temperature oxidation process of carbon-carbon composite materials (CCCM) with a pyrocarbon matrix has been examined. Oxidation at temperatures of 450 to 700 °C is characterized by internal burnout of the carbon phase without a noticeable change in the experimental samples external volume. Oxidation resistance analysis of CCCM structural components was performed. CCCM and carbon fibers specific surface area were estimated by the low-temperature adsorption of nitrogen and krypton using the Brunauer–Emmett–Teller model and the theory of density functional model. Pore size distribution was calculated by the semi-empirical Horvath–Kawazoe method. A significant increase (about 10-15 times) in specific surface area of the composite material, together with a rise in free volume ~5%, was accompanied by total weight loss of about 5%. Specific surface area changes occur as a result of anisotropic etching of carbon fibers surface with the formation of micropores with 0.5–2.0 nm diameter range. Although macropores are formed mainly due to the oxidation of thermosetting binder pyrolysis residue, they do not contribute to the specific surface increase but solely provide access to micropores. Microporosity evolution leads to an increase of structural discontinuity degree and, ultimately, to the loss of matrix-filler contact boundary. As a result, an

DOI: 10.52571/PTQ.v17.n34.2020.817_P34_pgs_793_802.pdf

overall weakening of material mechanical characteristics is to be noted. Thus, oxidative degradation is closely related to the increase in void space. A follow-up study is on-going. In fact, an open question remains, namely whether the oxidative process occurs differently in the micropores of diameter less than 2 nm and how it may contribute to the oxidative stress resistance behavior of CCCM.

Keywords: *oxidation, micropores, BET, DFT, CCCM, specific surface area.*

АННОТАЦИЯ

Исследован процесс низкотемпературного окисления углерод-углеродных композиционных материалов (УУКМ) с пироуглеродной матрицей. Окисление при температурах от 450 до 700 °C характеризуется внутренним выгоранием углеродной фазы без заметного изменения внешнего объема экспериментальных образцов. Проведен анализ стойкости к окислению структурных компонентов УУКМ. Удельная поверхность УУКМ и углеродных волокон оценивалась методом низкотемпературной адсорбции азота и криптона с использованием модели Брунауэра–Эммета–Теллера и теории функционала плотности. Распределение пор по размерам было рассчитано полуэмпирическим методом Хорвата–Кавазое. Значительное увеличение (примерно в 10-15 раз) удельной поверхности композиционного материала вместе с увеличением свободного объема ~5% сопровождалось общей потерей массы около 5%. Изменение удельной площади поверхности происходит в результате анизотропного травления поверхности углеродных волокон с образованием микропор диаметром 0,5 – 2,0 нм. При этом макропоры, образующиеся главным образом за счет окисления пиролизного остатка термореактивного связующего, не способствуют увеличению удельной поверхности, а лишь обеспечивают доступ к микропорам. Эволюция микропористости приводит к увеличению степени структурной неоднородности и в конечном итоге к потере контакта на границе матрица-наполнитель. В результате следует отметить общее ослабление механических характеристик материала. Таким образом, окислительная деградация приводит к увеличению пористости. В настоящее время исследование продолжается. На самом деле остается открытым вопрос, а именно, происходит ли окислительный процесс в микропорах диаметром менее 2 нм другим образом, и как этот процесс влияет на устойчивость УУКМ к окислению.

Ключевые слова: *окисление, микропоры, БЭТ, DFT, УУКМ, удельная поверхность.*

---

1. INTRODUCTION

Carbon-carbon composite materials (CCCM) are the basis for the creation of aerospace products that are operated under supercritical thermal, mechanical, and aerogasodynamic loads (Jin *et al.*, 2018; Terentieva *et al.*, 2011; Astapov and Terentieva, 2016; Yurishcheva *et al.*, 2018). The main task in the technology of super-temperature carbon materials is to provide effective protection against oxidation under conditions of high-velocity flow around high-enthalpy flows of oxygen-containing gases (Astapov and Rabinskiy, 2017; Terentieva and Astapov, 2018; Astapov *et al.*, 2019a; Astapov *et al.*, 2019b). Along with thermal spraying processes, chemical vapor deposition, and chemical vapor infiltration (Jin *et al.*, 2018; Yurishcheva *et al.*, 2018; Kiryukhantsev-Korneev *et al.*, 2017; Kiryukhantsev-Korneev *et al.*, 2018), slip protection coatings are widely used to protect CCCM (Astapov and Terentieva, 2016; Terentieva and Astapov, 2018; Astapov *et al.*, 2019a; Kablov *et al.*, 2017; Bankovskaya *et al.*, 2018).

The known technical solutions based on silicide, boride, carbide systems, and their compositions, as a rule, provide CCCM protection from oxidation above 1200-1300 °C and are ineffective below 700 °C. The boron oxide coatings (McKee, 1986) and phosphorus oxide coatings (Luthra, 1988) inhibit the diffusion of oxygen at low temperatures but evaporate or interact with carbon phase above 1000 °C. The lack of a unified approach to protecting CCCM consists in a complex oxidation mechanism, which depends on a number of parameters: (i) ambient temperature, (ii) oxygen partial pressure, (iii) nature of the oxidizing agent, (iv) structure and chemical composition of the carbon phase, and (v) mechanical stresses at the phase boundary. CCCM is an architecturally complex material represented by the following phases: (i) graphitized carbon fibers (CF), (ii) amorphous pyrolysis residue (PR) of a thermoset or pitch binder, and pyrocarbon (PC) matrix, whose structure depends on the regimes and hardware design of the deposition process. The CF properties substantially influenced by the precursor, the carbonization conditions, and the degree of graphitization.

The impact of the listed factors for oxidation resistance of CCCM estimated through analysis of porosity, specific surface area, and macrokinetics parameters of rate-controlling step at chemical and physical processes. Indicative in this regards are the works (Swaminathan-Gopalan *et al.*, 2019; Swaminathan-Gopalan *et al.*, 2018) devoted to mathematical modeling of the adsorption mechanism FiberForm® CF bulk oxidation, taking into account the evolution of their porous surface. The physical meaning for the dimension of the carbon oxidation rate constant by adsorbed oxygen atoms corresponds to the dimension of the specific surface per unit time reduced to the molar concentration [m^2/mol×sec].

The specific surface of carbon materials depends on the structure and production technology. For nanoscale forms of carbon (nanotubes, graphene), the specific surface area exceeds 2000 m^2/g; for catalysts, activated carbons, and soots, it is 500–1500 m^2/g. Pyrographite and glassy carbon are characterized by a minimal specific surface area and the lack of open porosity, its the reason for their resistance to oxidation up to 700 °C (Appen, 1976). The porosity nature of the phase carbon graphitized has a distinctive feature. According to the IUPAC classification (Dubinina, 1953; Dubinina, 1958), the pores forming the specific surface are mainly represented by slit micropores with a size of 0.5–2 nm. Amorphous forms of carbon show a wide variety of pores in size (micro-, meso-, macropores) and morphology: cylindrical, bottle-shaped, and spherical.

The study of the formal kinetics of CCCM oxidation is complicated by its heterophasic nature. CCCM structural components are characterized by different oxidative stability. Hence, the calculated values of the rate constant, activation energy, the oxidation reaction order are additive indicators and can not correspond to real values. Therefore, set up true mechanism CCCM heterogeneous oxidation, the staging, nature of the ongoing processes, and their mutual influence is really a difficulty. For example, the kinetics of the carbon materials oxidation at various conditions has been studied in detail for CF of varying degrees of graphitization (Govorov *et al.*, 2015), graphite (Rosner and Allendorf, 1965), C/SiC composites, and PC (Halbig, 2004). The rate constants, activation energy values, and the order of reactions are established. In the research of Ismail (1991), the nature of the change in the specific surface area of CF of various manufacturers during the oxidation process was examined in detail, the volume and size of micropores of various morphologies were estimated, and the effect of alkali metals on the oxidation kinetics at temperatures of 500-950 °C was studied At the present time, the region of reaction flowing for carbon materials heterogeneous oxidation have been determined depending on the temperature and oxygen pressure.

Despite the complete quantitative description for the oxidation kinetics and the extensive results in mathematical modeling ongoing processes, a number of questions remain that cause active discussions. The S-shaped kinetic profile at 450-700 °C indicates a complex mechanism with an induction effect or the autocatalysis phenom in the oxidation of CF and carbon composites with PC or ceramic matrix (Naslain *et al.*, 2004; Kumar and Kandasubramanian, 2019). A disadvantage in a complete understanding of the reaction mechanism and key factors affecting the oxidation rate limits the use of carbon materials in oxidizing media.

Due to the heterogeneous nature of the CCCM oxidation process, one of the main parameters determining its rate is the value boundary of the phase interface through which mass transfer proceeds (Kamyar *et al.*, 2019; Lee *et al.*, 2019). The complex influence of phase boundary consists of the fact that its only active part, the proportion of which varies with time, is involved in the process of low-temperature oxidation. Moreover, these changes are non-linear and difficult to predict. Therefore, conducting studies of structural changes in the surface and obtaining quantitative estimates is an urgent task for understanding and refining the mechanism of carbon materials oxidation.

The purpose of this work was to study structural changes in the CCCM carbon phase at the initial stages of low-temperature oxidation by estimating the specific surface area and analyzing the microstructure.

2. MATERIALS AND METHODS

A CCCM with a PC matrix INCARBO® (Russia) was used as the object of study. The CCCM was obtained on the basis of a carbon fabric CF UKN-M-3K (LLC Argon, Russia) based on polyacrylonitrile (PAN) precursor. The main characteristics of CF are presented in Table 1.

The prepregs were obtained by layering, and the phenol-formaldehyde resin was used as a binder. After the resin carbonization (binder mass loss was 40 wt.% at 1100 °C), PC bulk impregnation was carried out in methane medium at a residual pressure of 10-40 mm Hg in four cycles for 8 hours at 1300-1600 °C. The check was carried out by changing the mass of the workpiece at each stage of the technological redistribution.

The PC phase was obtained by the deposition of films with a thickness of 3–4 mm on an isostatic graphite substrate at a temperature of 1600 °C and a methane pressure of 30–40 mm Hg. The films were separated from the substrate by thermal shock. The determination of the porosity and the apparent CCCM density was carried out by hydrostatic weighing according to GOST R ISO 12985-2-2014 (ISO 12985-2: 2000). The weighing of the samples was carried out on an analytical balance GR-202 (AND, Japan) with an accuracy of 10^{-4} g. The CCCM samples were oxidized in an LHT04/17 SW chamber furnace (Nabertherm, Germany) with a working volume of 4 under isothermal conditions. The thermocouple TPR (type B) acted as a temperature sensor. Weighed samples in corundum boats were loaded into a furnace heated to operating temperature, kept at the isotherm for a predetermined time, cooled together with the furnace to 20 °C, removed from the furnace, and re-weighed. The oxidation was carried out in an air duct and in a mixture of air with helium at a flow rate of 70–220 ml/min.

The oxidation kinetics of CCCM, CF, and PC were studied by synchronous thermal analysis using an STA 449 F3 Jupiter instrument (Netzsch, Germany) in the thermogravimetric mode together with the differential scanning calorimetry mode on the isotherm. The samples were heated in open crucibles from Al_2O_3 with a volume of 0.085 ml at a linearly increasing furnace temperature at a rate of 20 °C/min. The oxidation was carried out in the air and in a mixture of air and helium at a gas flow rate of 70–220 ml/min. An empty crucible was used as a reference. The temperatures of the sample and the reference were measured using built-in S-type thermocouples made of Pt-Rh alloys. The change in mass of the samples was recorded with an accuracy of 1 µg. The balance drift over the entire temperature range did not exceed 10 mg/h.

For oxidation in a furnace, samples with sizes of 26.4×26.4×2.8 mm and 4.0×60×2.8 mm were used, and for thermal analysis, samples with sizes of 4.0×3.6×2.8 mm were used. Dried air supplied from a high-pressure cylinder through a desiccant was used as an oxygen source. Due to the low carbon dioxide content (0.03 vol.%), the effect of CO_2 on the oxidation reaction rate and chemical interaction with the carbon phase was neglected. Helium gas was used with a purity of 99.99999 vol.% (grade 7.0). To quantify the rate of mass loss, it was used the change in the mass of the sample as a result of the oxidation per unit of time with respect to the initial mass, [g/g×sec]. When analyzing volumetric bodies, it is customary to use the concept of the volumetric surface [m^{-1}], but since the quantitative assessment of the oxidation reaction was a change in mass, it was used the concept of a specific surface, reduced to the mass of the sample, [m^2/g]. The value of the total surface S_{tot} was expressed according to the measurement data through the product of the specific surface S_{sp} determined by the Brunauer-Emmett-Teller (BET) method and the mass of the sample.

The specific surface area of CCCM and CF were determined by the adsorption of nitrogen and krypton using the single point BET method on three independent devices: NOVA 1000e (Quantachrome Instruments, USA), Sorbi®-MS (META LLC, Russia), ASAP 2020 Plus Physisorption (Micromeritics, USA), and according to the density functional theory (DFT) by the quantum-chemical method of modeling adsorption on heterogeneous surfaces on an ASAP 2020 Plus Physisorption device (Micromeritics, USA). In this case, a graphite surface model with slit-like pores was used for calculations. Various ways for determining the specific surface, which were described above, were used due to the fact that, according to the BET theory, it is very difficult to obtain objective results in the presence of micropores (Rouquerol *et al.*, 1999). According to the results of calculations using DFT, the pore size distribution was obtained by the semi-empirical Horvath–Kawazoe method. The optical microscopy of the samples was performed in bright field mode using an inverted Olympus GX51 microscope (Olympus Life Science GmbH, Germany). The microstructural studies were performed on a Zeiss Supra 40VP scanning electron microscope (Carl Zeiss Group, Germany) in the secondary electron mode at an accelerating voltage of 10 kV and a beam current of 445 pA.

3. RESULTS AND DISCUSSION:

Figure 1 shows the mass loss data for low-temperature oxidation of CF of the UKN-M-3K grade, CCCM with PC matrix (CC), and PC phase. The obtained results for CF of the UKN-M-3K grade are in good agreement with the data on the oxidation of CF of the T-300 grade given in (Halbig, 2004). Despite the low oxidative stability of CF, the mass loss for CCCM based on them is much lower. According to the calculation of the activation energy of the CCCM oxidation reaction (Fig. 1), CF and, a carbonized PR of phenol-formaldehyde resin is predominantly oxidized. According to the optical microscopy, the cross-sectional structure of the initial CCCM samples with a PC matrix is relatively solid - without shells and voids (Fig. 2, b, c). However, numerous cracks were revealed on the surface of the samples (Fig. 2, a). They result from the relaxation of thermal stresses arising at the pyro-densification stage due to the difference in the linear thermal expansion coefficients of the CF and PC matrices in combination with a high modulus of elasticity and low CF elongation.

With a total CCCM mass loss due to oxidation of about 5% (Table 2), there were no visual changes in the structure of the surface layer (Fig. 2, *d*). No traces of oxidation were detected on the PC matrix surface. In volume, burnup occurs along the “CF–PR–PC” phase boundary and is accompanied by the formation of air channels oriented along CF (Fig. 2, *f*). The reason for this is the low oxidative stability of the amorphous PR low-temperature binder - phenol-formaldehyde resin. The oxidation of the PC matrix is less pronounced, since the oxidative stability of PC is higher, as can be seen from the data presented in Fig. 1. The analysis of the optical microscopy data allowed to say that, during low-temperature oxidation, the linear dimensions and volume of the samples remain almost unchanged. The change in density and porosity during the oxidation process occurs due to the loss of CF mass, binder residues, and the opening of closed pores. Table 2 summarizes that the values of apparent density and open porosity after the oxidation are proportional to mass loss. With a total mass loss of about 5%, the proportion of the free volume of the samples increased by almost 5%. Based on this, one can understand that the fraction of closed macropores in the CCCM structure is insignificant. This is consistent with the microscopy data.

The established increase in the specific surface area of CCCM during the low-temperature oxidation (Table 2) is an unobvious and important circumstance. Under the assumption that the geometrical dimensions of the samples remain unchanged during oxidation, the area of their external surface S_{ext} remains constant. However, the value of the total surface S_{tot}, taking into account both the external and internal (concentrated in the material pores) surface, undergoes significant changes. The calculated data on the total surface of CCCM samples before and after oxidation, obtained through the product of the specific surface S_{sp} (Table 2) by the corresponding mass of the sample, are presented in Table 3. It is possible to note that, as a result of oxidation, the total surface of CCCM increases by order of magnitude relative to its value for the initial samples and differs by four orders of magnitude from the surface area. Thus, as a result of the increase in the inner surface of the CCCM, its outer surface becomes a negligible value in comparison with the surface concentrated in micropores.

The works of K.L. Luthra (1988) and P.L. Walker *et al.* (1959) contain the results of attempts to make estimates of the specific surface area of carbon materials through their porosity. The most objective estimates of the change in the specific surface during CF oxidation are given by M.K.I. Ismail (1991). It was shown (Ismail, 1991) that in some cases, the specific surface area of CF can increase up to 60 m^2/g, while for CCCM, according to our data (Table 2), its increase is less pronounced. The oxidation of CCCM is a heterogeneous process. Therefore, it is supposed to bring the calculated reaction rate to the interface through which chemical interaction and mass transfer are carried out. With a significant difference in the external and volume surfaces (10^3–10^4 times), the influence of macrokinetic parameters on the oxidation rate at temperatures below 700 °C must be estimated, taking into account the nature of the change in specific surface.

The reason for the increase in the specific surface during oxidation and the total weight loss of the samples is the formation of micro- and mesopores with sizes of 0.5–2 nm and 2–50 nm (according to the IUPAC classification (Dubinina, 1953; Dubinina, 1958)), respectively. Macropores do not contribute to the specific surface; they provide access to meso- and micropores. Analyzing the oxidation resistance of the structural components of CCCM, one can conclude that macropores are formed as a result of oxidation of PR phenol-formaldehyde resin, and micro- and mesopores are formed as a result of oxidation of the CF surface. Such selective oxidation of CCCM breaks the contact at the "matrix–filler" interface. Therefore, control of the specific surface will allow an assessment of the kinetic stability of composite materials during oxidation.

Since the BET theory does not take into account the phenomenon of condensation of adsorbed gas in micropores (Rouquerol *et al.*, 1999; Carrot *et al.*, 1987), when they are present in the structure of the samples, the measurement results are distorted relative to reality. Therefore, the obtained data on the specific surface of CCCM (Table 2) were refined by the DFT calculation data and on the equipment of various manufacturers. The study was conducted on CCCM samples and individual CF. The measurement data averaged over four samples in each series are presented in Table 4. One can see that the specific surface values, according to BET and DFT, differ significantly. This is probably due to the presence of micropores on the CF surface. The BET data measured on NOVA 1000e and Sorbi®-MS showed good convergence. Additionally, according to DFT, the pore size distribution was calculated using the semi-empirical Horvath–Kawazoe method. The resulting estimates for CCCM after oxidation are shown in Table 5.

The microstructural heterogeneity of the studied objects and the significant measurement errors associated with it make it difficult to obtain reliable quantitative estimates of the specific surface area and pore distribution. However, qualitative changes in the structure of carbon materials during low-temperature oxidation are clearly visible. So, the BET specific surface area changes that we established (Tables 2, 4) are not consistent with the oxidation scheme proposed by M.C. Halbig (2004). According to Halbig`s scheme, CF degradation in the composite matrix proceeds uniformly - with a decrease in the fiber cross-section and correlates with mass loss. As a result, the specific surface area of the reinforcing CF is reduced during the oxidation process. That is, the model proposed by Halbig (2004) takes into account only the macroporosity of the C/SiC composite and does not consider possible changes in the specific surface. At the same time, the nature of structural changes during micro- and macroporosity differs fundamentally.

In view of the noted difficulties in assessing the specific surface area and pore size distribution, additional studies of CCCM samples were carried out before and after oxidation using scanning electron microscopy. The results are selectively presented in Figure 3. It can be seen that CF after CCCM oxidation has a more relief microstructure with a developed surface in comparison with a smoother surface of the initial fibers. This indirectly indicates the effect of etching the CF surface with oxygen, accompanied by the appearance of microcavities and ledges. The formation of mesopores 2–50 nm in size is not observed; the presence/absence of micropores has not been visually established due to insufficient resolution of the microscope. This result is not consistent with the obtained pore size distribution data (Table 5). Apparently, the heterophase structure of the composite material affects the results of measurements of the specific surface and data on the distribution and volume of micropores.

The formation of micropores in the process of low-temperature oxidation is possible by several mechanisms. According to Ismail (1991), a CF structure is characterized by closed microporosity; as the surface oxidizes, the pores open, and the specific surface increases. The most likely explanation for the appearance of micropores is proposed by K.L. Luthra (1988), as an anisotropic etching of the CF surface. The reasons for the manifestation of anisotropy and the mechanism of the appearance of micropores with boundary sizes of 0.8-1.2 nm (Ismail, 1991) are poorly studied and constitute a subject for future scientific discussion. The most plausible hypothesis seems to be expressed by Naslain *et al.* (2004) and Walker *et al.* (1959). Anisotropic oxidation of the carbon surface is due to defects in the structure of the fiber and the presence of impurities. It becomes apparent to a lesser extent as the degree of graphitization of the carbon phase of the fibers increases.

Thus, the low-temperature degradation of CCCM is due to an increase in the number of micropores on the CF surface. As a result, with a slight loss of mass, a substantial increase in the volume surface is observed. Its value is 10^3–10^4 times greater than the external surface area. At the macro level, the contact between the PC matrix and CF is broken in the structure of the composite material. This, together with an increase in the degree of structural discontinuity as a result of the formation and development of microporosity, leads to a decrease in the work aimed at breaking the binding forces in the "fiber–matrix" system and the work of pulling out the fibers from the matrix. The consequence is a decrease in the mechanical properties of CCCM both at room temperature (tensile strength, yield strength) and at elevated temperatures (creep strength, tensile strength).

4. CONCLUSIONS:

The oxidation of CCCM based on PAN fibers with a PC matrix at temperatures of 450 to 700 °C is voluminous and is accompanied by a significant change in porosity and specific surface with no visible signs of oxidation from the outside. The process of low-temperature oxidation of CCCM is anisotropic in nature at the macro- and microstructural levels. At the macro level, this is manifested in various oxidative stability of the structural components of the composite material - CF, PC matrix, and PR thermosetting binder. At the micro-level, this is manifested by anisotropic etching of the CF surface, accompanied by an increase in microporosity. Macropores do not contribute to the value of the specific surface, but only provide access to meso- and micropores.

The oxidation of CCCM proceeds predominantly along the CF–PR–PC phase boundary and results in the rupture of the contact between the matrix and the filler. This, together with an increase in the degree of structural discontinuity due to the formation and development of microporosity, leads to a decrease in the kinetic stability of the composite material and the loss of its mechanical properties.

5. ACKNOWLEDGMENTS:

This work was carried out as part of the RSF grant for the event “Research by scientific groups led by young scientists” of the Presidential Program for Research Projects (Agreement No. 19-79-10258 of 08.08.2019).

6. REFERENCES:

1. Appen, A.A. *Temperature-resistant inorganic coatings*, Leningrad: Khimiya, **1976**.
2. Astapov A.N., Rabinskiy, L.N. *Solid State Phenomena*, **2017**, *269*, 14-30. DOI: 10.4028/www.scientific.net/SSP.269.14.
3. Astapov, A.N., Lifanov, I.P., Rabinskiy, L.N. *High Temperature*, **2019a**, *57*(5), 744-752. DOI: 10.1134/S0018151X19050018.
4. Astapov, A.N., Terentieva, V.S. *Russian Journal of Non-Ferrous Metals*, **2016**, *57*(2), 1-173. DOI: 10.3103/S1067821216020048.
5. Astapov, A.N., Zhestkov, B.E., Lifanov, I.P., Rabinskiy, L.N., Terentieva, V.S. *Arabian Journal for Science and Engineering*, **2019b**, *44*(6), 5323-5334. DOI: 10.1007/s13369-018-3585-4.
6. Bankovskaya, I.B., Nikolaev, A.N., Kolovertnov, D.V., Polyakova, I.G. *Physics and Chemistry of Glass*, **2018**, *44*(5), 509-515. DOI: 10.7868/S0132665118050086.
7. Carrot, P.J.M., Roberts, R.A., Sing, K.S.W. *Carbon*, **1987**, *25*(1), 59-68. DOI: 10.1016/0008-6223(87)90040-6.
8. Dubinina, M.M. Methods for studying the structure of finely dispersed and porous bodies. *Proceedings of the Meeting*, July 25-29; Moscow, Russia, **1953**, 164-166.
9. Dubinina, M.M. Methods for studying the structure of finely dispersed and porous bodies. *Proceedings of the Second Meeting,* June 13-18; Moscow, Russia, **1958**, 296-298.
10. Govorov, A.V., Galiguzov, A.A., Tikhonov, N.A., Malakho, A.P., Rogozin, A.D. *New Refractories*, **2015**, *11*, 34-39.
11. Halbig, M.C. Oxidation kinetics and strength degradation of carbon fibers in a cracked ceramic matrix composite. *28th International Conference on Advanced Ceramics and Composites B: Ceramic Engineering and Science Proceedings*, January 25-30; Florida, USA, **2004**, 137-146.
12. Ismail, M.K.I. *Carbon*, **1991**, *29*(6), 777-792. DOI: 10.1016/0008-6223(91)90017-D.
13. Jin, X., Fan, X., Lu, C., Wang, T. *Journal of the European Ceramic Society*, **2018**, *38*(1), 1-28.
14. Kablov, E.N., Zhestkov, B.E., Grashchenkov, D.V., Sorokin, O.Yu., Lebedeva, Yu.E., Vaganova, M.L. *Thermophysics of High Temperatures*, **2017**, *55*(6), 704-711. DOI: 10.7868/S0040364417060059.
15. Kamyar, N., Rezaee, S., Shahrokhian, S., Amini, M.M. *Journal of Colloid and Interface Science*, **2019**, *555*, 655-666.
16. Kiryukhantsev-Korneev, Ph.V., Iatsyuk, I.V., Shvindina, N.V., Levashov, E.A., Shtansky, D.V. *Corrosion Science*, **2017**, *123*, 319-327. DOI: 10.1016/j.corsci.2017.04.023.
17. Kiryukhantsev-Korneev, Ph.V., Potanin, A.Yu. *Russian Journal of Non-Ferrous Metals*, **2018**, *59*(6), 698-708. DOI: 10.3103/S106782121806010X.

18. Kumar, C.V., Kandasubramanian, B. *Industrial and Engineering Chemistry Research*, **2019**, *58*(51), 22663-22701.

19. Lee, S., Park, G., Kim, J.G., Paik, J.G. *International Journal of Aeronautical and Space Sciences*, **2019**, *20*(3), 620-635.

20. Luthra, K.L. *Carbon*, **1988**, *26*(2), 217-224. DOI: 10.1016/0008-6223(88)90040-1.

21. McKee, D.W. *Carbon*, **1986**, *24*(6), 737-741. DOI: 10.1016/0008-6223(86)90183-1.

22. Naslain, R., Guette, A., Rebillat, F., Le Gallet, S., Lamouroux, F., Filipuzzi, L., Louchet, C. *Journal of Materials Science*, **2004**, *39*(24), 7303-7316. DOI: 10.1023/B:JMSC.0000048745.18938.d5.

23. Rosner, D.E., Allendorf, H.D. *Carbon*, **1965**, *3*(2), 153-156. DOI: 10.1016/0008-6223(65)90042-4.

24. Rouquerol, F., Rouquerol, J., Sing, K. *Adsorption by powders and porous solids,* Cambridge: Academic Press, **1999**. DOI: 10.1016/B978-0-12-598920-6.X5000-3.

25. Swaminathan-Gopalan, K., Borner, A., Murray, V.J., Poovathingal, S., Minton, T.K., Mansour, N.N., Stephani, K.A. *Carbon*, **2018**, *137*, 313-332. DOI: 10.1016/j.carbon.2018.04.088.

26. Swaminathan-Gopalan, K., Stephani, K.A., Ferguson, J., Borner, A., Panerai, F., Mansour, N.N. Effective oxidation model for light-weight carbon preform ablators. *AIAA SciTech Forum*, January 7-11; San Diego, USA, **2019**, 63-67.

27. Terentieva, V.S., Astapov, A.N. *Russian Journal of Non-Ferrous Metals*, **2018**, *59*(6), 709-718.

28. Terentieva, V.S., Eremina, A.I., Astapov, A.N., Leipunskii, I.O., Pshechenkov, P.A. *Composites: Mechanics, Computations, Applications*, **2011**, *2*(3), 247-270.

29. Walker, P.L. Jr., Rusinko, F. Jr., Austin, L.G. Gas reactions of carbon. In Eley, D.D., Selwood, P.W., Weisz, P.B. (Eds.): *Advances in Catalysis. Vol. 11* (pp. 133-221), New York: Academic Press, **1959**.

30. Yurishcheva, A.A., Astapov, A.N., Lifanov, I.P., Rabinskiy, L.N. *Key Engineering Materials*, **2018**, *771*, 103-117. DOI: 10.4028/www.scientific.net/KEM.771.103.

Table 1. *Properties of the CF UKN-M-3K based on the PAN precursor*

Linear density, tack	190
The diameter of the filament, μm	7
Modulus of elasticity, GPa	225
Specific breaking load at the break of a loop, cN/tack	10
Tensile stress, GPa	3.5
Density, g/cm^E	1.75
Processing temperature, °C	1500
A specific surface according to BET, m^2/g	1.35

Table 2. *The apparent density ρ_{app}, open porosity P_o and specific surface area S_{sp} by BET (NOVA 1000e) of CCCM samples in the initial state and after oxidation at T = 570°C, PO_2 = 0.6 atm for 190 min*

No.	**Mass loss, %**	**ρ_{app}, g/cm^3**		**P_o, %**		**S_{sp}, m^2/g**	
		Before oxidation	**After oxidation**	**Before oxidation**	**After oxidation**	**Before oxidation**	**After oxidation**
1	-4.985	1.52	1.46	2.6	7.8	1.18	14.26
2	-4.801	1.50	1.46	2.7	7.4	1.07	14.39
3	-3.922	1.51	1.47	2.7	7.4	1.15	13.62
4	-4.839	1.52	1.46	2.7	7.7	1.01	13.87

Table 3. *The calculated data on the total surface area of CCCM samples by BET in the initial state and after oxidation at T = 570°C, PO2 = 0.6 atm for 190 min*

No.	**Sample mass, g**		**External surface S_{ext}, cm^2**	**Total surface S_{tot}, cm^2**	
	Before oxidation	**After oxidation**		**Before oxidation**	**After oxidation**
1	0.983	0.934	8.077	11599.4	133188.4
2	1.083	1.031	8.991	11588.1	148360.9
3	0.969	0.931	8.016	11143.5	126802.2
4	1.054	1.003	8.644	10645.4	139116.1

Table 4. *Data on the specific surface area of samples by nitrogen adsorption (CCCM) and krypton adsorption (CF)*

Sample	**Specific surface S_{sp}, m^2/g**	**BET**			**DFT**
		NOVA 1000e	**Sorbi®-MS**	**ASAP 2020 Plus Physisorption**	
CCCM	Before oxidation	1.3	1.2	<1	-
	After oxidation At *T* = 570°C (mass loss 5%)	14.0	13.0	10.5	7.5
CF	Before oxidation	0.8	<1	<1	-
	After oxidation At *T* = 570°C (mass loss 5%)	29.4	32.1	24.6	19.6

Table 5. *Pore size distribution for CCCM after oxidation at T = 570 ° C (mass loss 5%) obtained by the semi-empirical Horvath–Kawazoe method*

Volume available for gas adsorption – 0.01 cm^3/g	0.5–2 nm micropores	2–50 nm mesopores
Share, %	25–35	65–75

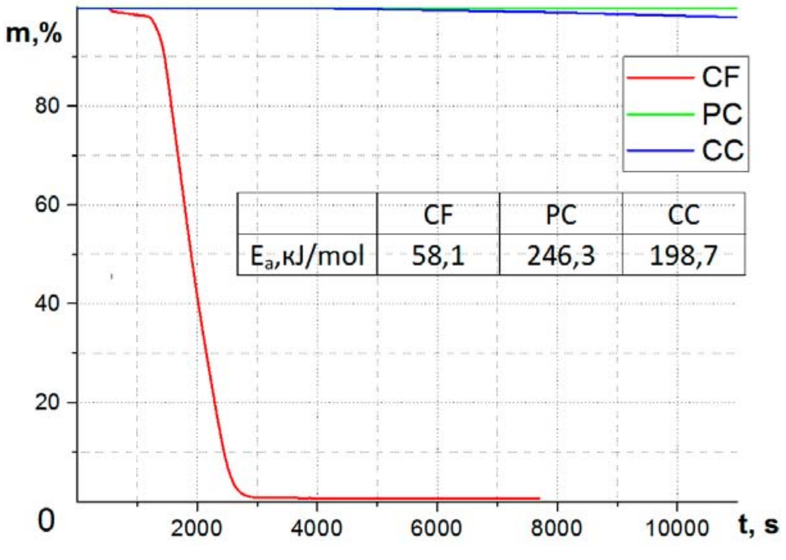

Figure 1. *Data on mass loss during oxidation at T = 570°C, PO2 = 0.6 atm for CF of the UKN-M-3K grade, CCCM with PC matrix (CC), and PC phase (PC)*

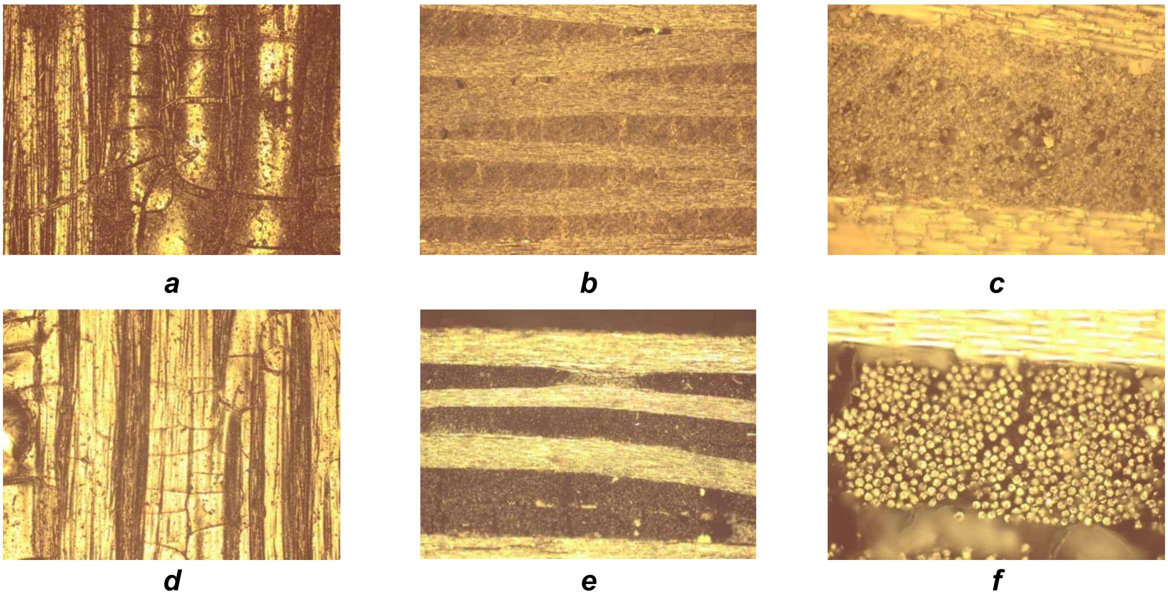

Figure 2. *The structure of CCCM according to optical microscopy in the initial state (**a**, **b**, **c**) and after oxidation at T = 570°C, PO2 = 0.6 atm for 190 min. (d, e, f): **a**, **d** - x50; **b**, **e** - x100; **c**, **f** - x500*

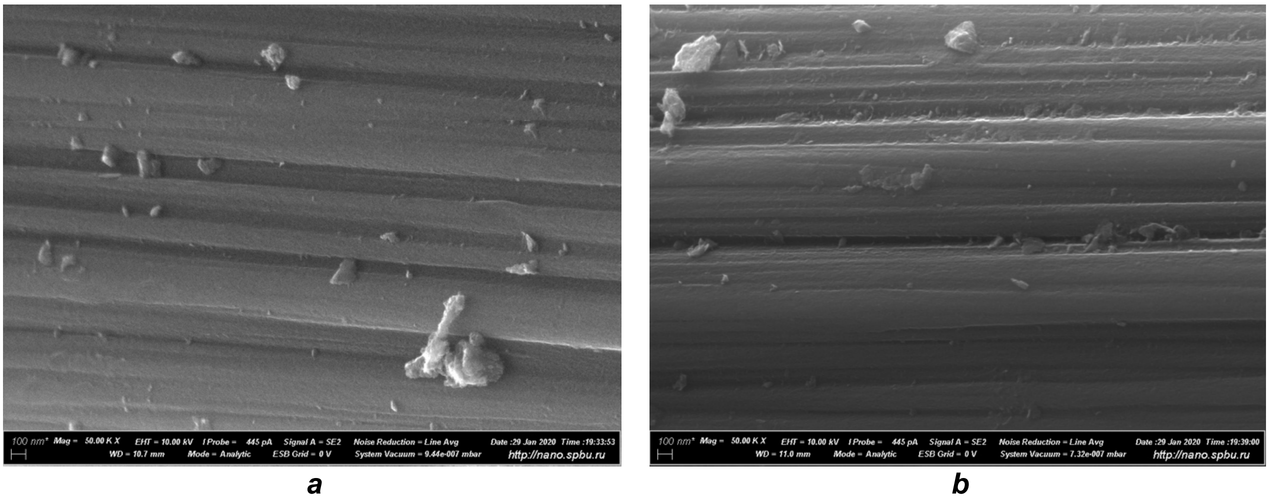

Figure 3. *Microstructure of CF in secondary electrons before (**a**) and after (**b**) oxidation of CCCM at T = 570°C (mass loss 5%)*